Terrain modelling of glideslope for instrument landing system

M.M. Poulose, MTech
P.R. Mahapatra, ME, PhD
N. Balakrishnan, BE, PhD

Indexing terms: Radio wave propagation (terrain effects), Radar and radionavigation

Abstract: The paper makes a contribution to the evaluation of irregularities introduced in electronically defined glideslopes of UHF instrument landing systems (ILS) by the unevenness of the terrain around the glideslope antenna. Various methods of physical and geometric optics have been applied in recent years to model and estimate the glideslope aberration at given locations prior to actual installation. A systematic study of various methods is made in the paper. A general treatment is evolved, which is capable of exhaustively handling arbitrary ray order effects and topography. The uniform asymptotic theory has been applied to the ILS problem and results compared with the uniform theory of diffraction. The results of actual case studies are presented.

1 Introduction

The Instrument Landing System (ILS) provides the pilot of an aircraft with steering information which enables him/her, even in poor conditions of visibility, to make an accurate and controlled runway approach and landing. The main constituents of the ILS are the localiser, glidepath and marker beacons [1, 2]. The localiser, operating in the 108–112 MHz band, provides azimuth guidance information through the differential depth of modulation (DDM) of two signals at 90 and 150 Hz. The DDM is zero along the centre line of the runway and varies linearly over the course sector. The elevation guidance is provided by the glideslope in the 328–336 MHz band, also operating on the DDM principle with 90 and 150 Hz tones.

An aircraft on or near the glideslope receives not only the direct signals from the antenna system but also signals reflected from the intervening terrain. The effect of reflection, which varies from location to location, must be taken into account in determining the shape of the electronic glideslope in the presence of a particular terrain. The design of the most widely used arrays for ILS is based on image theory in which the ground plane is idealised as being infinite and perfectly conducting. As the elevation angles involved are small and wavelengths fairly large, wide stretches of plane ground must be available in front of the antenna to obtain a reasonable approximation to the ideal image patterns.

Paper 5322H (E11, E15), first received 9th July and in revised form 28th November 1986

The authors are with the Department of Aerospace Engineering, Indian Institute of Science, Bangalore 560 012, India

The limited extent of the plane ground in front of the glidepath antenna usually results in what are known as 'course bends'. Initial attempts at terrain modelling for ILS glideslopes were based on physical optics (PO) [3–6]. The PO technique is based on assumed ground currents which are integrated to obtain the scattered field from the reflecting terrain. In this method, ground currents in one area are assumed to have no effect on the neighbouring areas. Such an assumption is necessary to determine the fields within a reasonable computation time. Thus the PO models allow the electric fields radiated by the ground to pass through any subsequent obstructions as if they do not exist.

A model developed by Godfrey *et al.* [7] was based on the half-plane diffraction solution of Senior [8], Woods [9], and Bromwich [10]. However, this model can handle only limited terrain configurations.

The excessive computational requirements of PO methods have led to the search for ray based or geometrical optic (GO) based theories [11]. The simplest application of GO to the study of terrain effects considers only the direct rays from the antenna and the reflected rays from the terrain. Although it can account for terrain slopes and reflectivity aspects, it results in discontinuities in the computed field in the presence of terrain drop-offs.

The geometrical theory of diffraction (GTD) developed by Keller [12, 13] overcomes the problem associated with GO methods by including the diffracted rays. However, in this formulation, the fields become infinite at the reflection and shadow boundaries, whereas far from these boundaries, the field prediction is accurate. This drawback has been overcome subsequently by the uniform theory of diffraction (UTD) [14, 15] and uniform asymptotic theory (UAT) [16, 17]. In the ILS glideslope application, the free-space vertical pattern of the particular antenna can be approximated by an isotropic source. For such a source, Rahmat-Samii and Mittra have shown that the UTD and UAT result in the same field estimates in the presence of a half plane [18]. However, there appear to be differences of opinion regarding the applicability and relative accuracy of the two methods [18, 19]. The conflict has not been satisfactorily resolved because, unlike the UTD, for which results have been available in the last few years [20–22], UAT has not yet been applied to any practical problems.

The methods enumerated above deal essentially with fields generated in the presence of individual terrain elements. Successful terrain modelling of real sites, extending over thousands of wavelengths, requires a large number of elements to be examined for their effects, including mutual interactions of high order. To keep the problem tractable, truncations and certain simplifying

assumptions are essential. Quite often these are done rather arbitrarily, based on experience. The current study makes an extensive and systematic assessment of the effect of various terms in each model and of the level of truncation on the overall accuracy/ease of computation tradeoff to lay a scientific basis for the systematic selection of the method of modelling and the threshold of truncation. In this paper, UAT is applied for the first time to a real ILS site to generate results and compare them with earlier methods and actual measurements.

2 Theory

The ILS image glideslope antenna system typically consists of two or three subarrays, each excited with an amplitude and phase depending on the type of the system used, namely null reference, sideband reference and *m*-array. The resultant field at an observation point may be obtained by the superposition of fields due to individual antenna elements, in the presence of reflecting terrain. This procedure, along with the algorithm for DDM computation, is detailed in the following Sections. A ray theoretical approach is made to the field computation, assuming the antenna element to be a point source.

2.1 Field computation

According to GTD the total field at an observation point is the sum of the GO and the diffracted fields; this can be represented as (see Fig. 1)

$$E^t_{s,h} = E^g_{s,h} + E^d_{s,h} = E_0\left[\frac{e^{-jks_0}}{s_0} \mp \frac{e^{-jks''}}{s''} + \frac{e^{-jks'}}{s'} D_{s,h} e^{-jks} A_d\right] \quad (1)$$

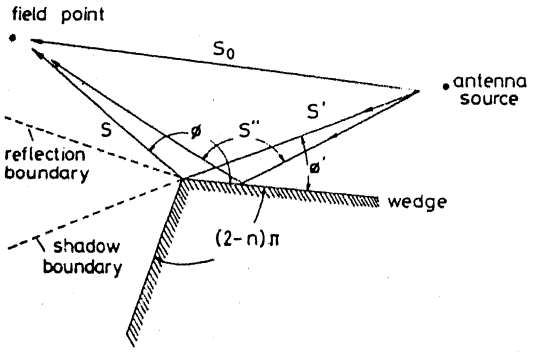

Fig. 1 *Diffraction and reflection at a wedge*

where the diffraction coefficient $D_{s,h}$ and the divergence factor A_d are given by Keller [13]:

$$D_{s,h} = \frac{-e^{-j\pi/4}\sin\frac{\pi}{n}}{n\sqrt{(2\pi k)}\sin\beta_0} \times\left[\frac{1}{\cos\frac{\pi}{n} - \cos\frac{\beta^-}{n}} \mp \frac{1}{\cos\frac{\pi}{n} - \cos\frac{\beta^+}{n}}\right]$$

and

$$A_d = \frac{s'}{s'(s+s')} \quad (2)$$

Eqn. 2 is not valid in the transition regions in the vicinity of shadow and reflection boundaries, where it predicts infinite fields.

The above drawback of the GTD has been overcome by the two uniform theories. In the UTD [13, 14] the diffraction coefficient in eqn. 2 is modified by introducing Fresnel and cotangent functions and is given by

$$D_{s,h} = \frac{-e^{-j\pi/4}}{2n\sqrt{(2\pi k)}\sin\beta_0} \times\left[\cot\left(\frac{\pi+\beta^-}{2n}\right)F[kLa^{\pm}\beta^-] + \cot\left(\frac{\pi-\beta^-}{2n}\right)F[kLa^{\mp}\beta^-] \pm\left\{\cot\left(\frac{\pi+\beta^+}{2n}\right)F[kLa^{\pm}_{+}\beta^+] + \cot\left(\frac{\pi-\beta^+}{2n}\right)F[kLa^{\mp}_{+}\beta^+]\right\}\right] \quad (3)$$

where

$$F(x) = 2j|\sqrt{x}|e^{jx}\int_{|\sqrt{x}|}^{\infty} e^{-\tau^2}\,d\tau \quad (3a)$$

$$a^{\pm}_{\pm} = 2\cos^2\left(\frac{2n\pi N^{\pm}_{\pm} - \beta^{\pm}}{2}\right) \quad (3b)$$

$N^{\pm}_{\pm}$ = integers which most nearly satisfy the following equations:

$$2\pi n N^{+}_{\pm} - \beta^{\pm} = \pi \quad (3c)$$

$$2\pi n N^{-}_{\pm} - \beta^{\pm} = -\pi \quad (3d)$$

and

$$\beta^{\pm} = \phi \pm \phi' \quad (3e)$$

The distance parameter for spherical wave incidence is given by

$$L = \frac{ss'}{(s+s')}\sin^2\beta_0 \quad (3f)$$

In UAT the diffracted field E^d is as in eqn. 2. The modified GO field E^{go} is given by [16, 17]

$$E^{go} = [F(\xi^i) - \hat{F}(\xi^i)]E^i + [F(\xi^r) - \hat{F}(\xi^r)]E^r \quad (4)$$

where

$$F(x) = \frac{e^{-j\pi/4}}{\sqrt{\pi}}\int_x^{\infty} e^{i\tau^2}\,d\tau \quad (4a)$$

$$\hat{F}(x) = \frac{1}{2x\sqrt{\pi}}e^{j(x^2+\pi/4)} \quad (4b)$$

$$\xi^i = \mp\sqrt{(k)}|(s'+s-s_0)^{1/2}| \quad (4c)$$

and

$$\xi^r = \mp\sqrt{(k)}|(s'+s-s'')^{1/2}| \quad (4d)$$

where the positive and negative signs correspond to the shadow and lit regions, respectively.

Both UTD and UAT formulations have been applied to the ILS problem in this paper.

2.2 DDM computation

The far field in front of the antenna may be represented by

$$E = A[1 + m\cos\omega_m t]\exp[i\omega_c t] \quad (5)$$

where

A = the field vector whose amplitude is inversely proportional to the distance from the antenna and phase directly proportional to the distance

m = the modulation index

ω_m = the modulating angular frequency

ω_c = the carrier angular frequency

The carrier-plus-sideband (CSB) and sideband only (SBO) fields in the ILS system are modulated at 90 and 150 Hz. Denoting these frequencies by ω_{90} and ω_{150} respectively, the field due to the CSB signal can be written as

$$E_{cs} = A_{cs}[1 + m(\cos \omega_{90} t + \cos \omega_{150} t)] \quad (6)$$

where the subscript '*cs*' refers to the CSB signal. Similarly, the field due to the SBO signal can be written as

$$E_{sb} = A_{sb} m[\cos \omega_{90} t - \cos \omega_{150} t] \quad (7)$$

where the subscript '*sb*' refers to SBO signal.

The total complex field envelope at the observation point (aircraft) is the sum of the CSB and SBO fields.

The detector at the aircraft receiver outputs a signal proportional to the amplitude of the total field envelope. The normalised detector output E_{od} can be represented as

$$E_{od} = |(E_{cs} + E_{sb})/A_{cs}| \quad (8)$$

Substituting for E_{cs} and E_{sb} from eqns. 6 and 7 and simplifying, eqn. 8 reduces to

$$E_{od} = [(1 + E_1)^2 + E_2^2]^{1/2} = [1 + 2E_1 + E_1^2 + E_2^2]^{1/2} \quad (9)$$

where

$$E_1 = m[1 + \text{Re}\,(A_{sb}/A_{cs})] \cos \omega_{90} t + m[1 - \text{Re}\,(A_{sb}/A_{cs})] \cos \omega_{150} t \quad (9a)$$

and

$$E_2 = \text{Im}\,(A_{sb}/A_{cs}) m \cos (\omega_{90} t - \omega_{150} t) \quad (9b)$$

Expanding eqn. 9 as a power series,

$$E_{od} = 1 + [(2E_1 + E_1^2 + E_2^2)/2] - [(2E_1 + E_1^2 + E_2^2)^2/8] + \text{higher order terms} \quad (10)$$

E_1 contains undistorted 90 and 150 Hz signals. E_1^2 and E_2^2 contain harmonics of the 90 and 150 Hz signals and their sums and differences. The third and higher order terms contain harmonics and cross product frequencies including some additional small amplitude 90 and 150 Hz signals. The detector output is passed through 90 and 150 Hz filters.

Neglecting the contributions from the 3rd- and higher-order terms, the outputs from these filters can be considered to come from E_1 in the second term of eqn. 10. Therefore, the outputs from the 90 and 150 Hz filters can be written as

$$E_{90} = m[1 + \text{Re}\,(A_{sb}/A_{cs})] \quad (11a)$$

and

$$E_{150} = m[1 - \text{Re}\,(A_{sb}/A_{cs})] \quad (11b)$$

The DDM signal is obtained by taking the difference between the E_{90} and E_{150} signals obtained above. The DDM is therefore given by

$$DDM = E_{90} - E_{150} = 2m\ \text{Re}\,(A_{sb}/A_{cs}) \quad (12)$$

Glidepath systems are normalised so that at $\pm 0{\cdot}35$ degrees relative to the desired path angle, the aircraft DDM indicator reads $\pm 75\,\mu$A. Thus the normalised DDM can be represented as

$$DDM_{\mu A} = \frac{\rho}{|\rho|_{0.35^\circ} + |\rho|_{-0.35^\circ}} \quad (13)$$

where

$$\rho = \text{Re}\,(A_{sb}/A_{cs}) \quad (13a)$$

and $|\rho|_{\pm 0.35^\circ}$ is the value of ρ at

$$\Delta\theta = \pm 0.35^\circ \quad (13b)$$

The value of the field contributions A_{sb} and A_{cs} due to the SBO and CSB antenna subarrays can be computed using the field computation methods given in the preceding Section.

In ILS handbook and operating literature, for instinctive understanding, formulas 12 and 13 are represented, respectively, as

$$DDM = 2m\ \text{Re}\,(SBO/CSB) \quad (14)$$

$$DDM_{\mu A} = 75\,\frac{\text{Re}\,(SBO/CSB)}{\frac{1}{2}[|\text{Re}\,(SBO/CSB)|_{\Delta\theta = 0.35^\circ} + |\text{Re}\,(SBO/CSB)|_{\Delta\theta = -0.35^\circ}]} \quad (15)$$

3 Modelling of the terrain

The terrain is modelled as piecewise planar, i.e. made up of connected flat plates whose edges are mutually parallel and perpendicular to the runway centre line. They are assumed to extend to infinity laterally, as shown in Fig. 2.

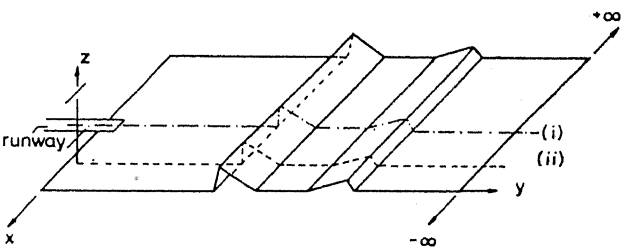

Fig. 2 *A schematic 7-plate wedge model for a typical ILS terrain*
(i) runway centre line
(ii) terrain profile line

The parameters of such a model may be constructed from a contour plan of the terrain or from aerial altimetry along the extended runway centre line.

4 Ray types, their existence and order effects

Determination of ray types is the first major step in the use of the ray theoretic approach for field evaluation in the presence of multiple wedges. While the earlier treatments of the subject are based on certain simplifying assumptions [20, 21] as far as the ray groups are considered, in this study we have developed algorithms which exhaustively test for the existence of rays of any order including all combinations. This means that the primary three ray types, namely direct (D), reflected (R), and diffracted (D_f) rays from each plate/edge can be combined in any order upto any level (e.g. D, R, D_f, DDR, RD_fD, DD_fD_f etc.), and the computer model would automatically check for the existence of the particular combination for the given antenna and observer location on the terrain model. For each ray that is found to exist, the model would proceed to compute the vector field contribution at the observer point.

Rays upto the 3rd-order have been considered in practical problems to show that exhaustive computation with as many as 12 plates can be accomplished with reasonable computer time (less than 5 s of CPU time on a DEC 1090 system for each observation point, i.e. about 5 minutes for a full 80-point glideslope segment).

5 Application to actual site

The model developed has been applied to the ILS installed at an existing airport in India. The operating frequency is 335.0 MHz and the antenna is offset by a distance of about 135 m from the runway centre line. The idealised (piecewise linearised) terrain profile through the antenna location is shown in Fig. 3.

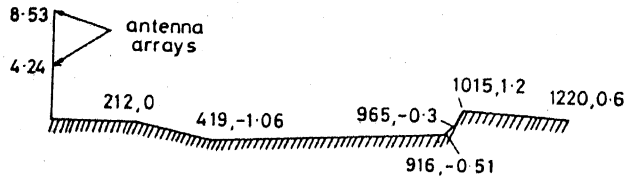

Fig. 3 *Six segment idealisation of the terrain profile line at an airport in India*
Co-ordinates are in metres (not to scale)

The wedges defining the terrain are assumed to be smooth and perfectly conducting. At grazing incidence angles, the assumption of perfect conduction is very close to reality. For the particular case of the wavelength considered here, this fact is supported by actual computations; some sample results are given in the concluding remarks at the end of this paper.

6 Results and discussion

As per International Civil Aviation Organisation (ICAO) standards [23], the flight validation process includes a level run and a low level approach for measuring the vertical and structural characteristics of the glideslope. The measured and computed curves for the DDM against elevation angle for a 1000 ft (305 m) level run are shown in Fig. 4*a* for the airport mentioned in Section 5. The various glideslope parameters are tabulated in Table 1.

Table 1: Measured and computed angle parameters in degrees

Parameter	Measured	UAT	UTD
Path angle	3.0	2.98	2.98
Total width	0.72	0.69	0.676
CPU time		92.6	69.34

The difference between the measured and computed (both UTD and UAT) angle is found to be only 0.02°. Against a total course width of 0.72°, the computed value is 0.69° for the UAT and 0.676° for the UTD, which also shows good agreement. Fig. 4*b* shows the computed and measured DDM against distance for a low level approach. The maximum offset is found to be 17 μA which is well within the tolerance limit set by the ICAO.

A point worth noting in the results represented by Figs. 4*a* and *b* as well as Table 1 is the high degree of agreement between the UTD and the UAT for the glideslope problem. As briefly mentioned in the penultimate paragraph of Section 1, there have been some differences of perception regarding the applicability and relative accuracy of the UAT. Although the results reported in this Section will not establish any of the viewpoints, which are primarily based on single-wedge geometries, it is hoped that they will make a contribution towards

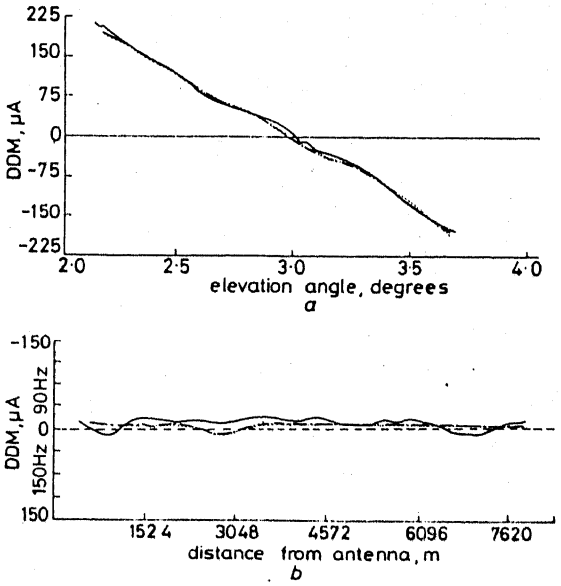

Fig. 4 *DDM at the airport profiled in Fig. 3*
a At various elevation angles for a 1000 ft (305 m) level run
b Along a nominal 3° glideslope run
——— measured
—·—· UTD calculated
····· UAT calculated

putting the UAT and UTD in proper perspective, especially in the case of relatively complex multiwedge geometries. For complex geometries, the overall effects are averaged out over the contribution due to many wedges, and, as found here, both the UAT and UTD are applicable and provide very close results.

7 Concluding remarks

The paper proposes a theory for the modelling of terrain effects on ILS glideslopes, and presents actual results demonstrating the validity of the model. This problem is of both theoretical elegance and high practical value because glideslope imperfections have in fact been linked to many air crashes. The experience gained from this study shows that sophisticated mathematical modelling cany yield results very close to true or measured data on the glideslope. Thus modelling can be a low cost, fast and versatile method of site evaluation for ILS installations.

As mentioned in Section 5, the terrain in front of the glideslope antenna has been assumed to be fully conducting. This assumption is necessitated by the application of the standard form of the UTD and UAT, and is justifiable for the low incidence angles involved in ILS applications. However, variants of the UTD which take into account surface impedance have been attempted [24, 25], and their application corroborates this view. For example, in Table 1, introducing a surface impedance of 30–*j*30 Ω (per square), corresponding to the terrain at the airport under consideration, changes the path angle to 3.0° and the course width to 0.70° as computed by the method in Reference 25. It is thus seen that the zero-impedance assumption is quite valid, though a small step in the right direction can be obtained by considering impedance effects, at the expense of much computation.

8 References

1 'Technical manual on ILS'. TP-3140, Plessey Radar, Addletone, UK, 1972

2 'Installation instruction for ILS'. DOT/FAA 6750.6A, US Federal Aviation Administration, 1969
3 MACFARLAND, R.H., HILL, D., and LUTTERMOSER, D.: 'Earth cover and contour effects on image glidepaths'. Final Report EER 5-1, Contract FA 64WA 5060, Avionics Research Group, Ohio University, OH, USA, 1968
4 RAMAKRISNA, S., and SACHIDANANDA, M.: 'Calculating the effect of uneven terrain on glidepath signals', *IEEE Trans.*, 1974, **AES-10**, pp. 380–384
5 MORIN, S., NEWSOM, P., KAHN, D., and JORDAN, L.: 'ILS glideslope performance prediction'. Report FAA-RD-74-157.A, Transportation Systems Centre, Cambridge, MA, USA, 1974
6 AAS, J.A.: 'Performance of advanced approach landing systems (AALS)'. NATO, ELAB, NTH, 1973
7 GODFREY, J.T., HARTLEY, H.F., MOUSALLY, G.J., and MOORE, R.A.: 'Terrain modelling using the half plane geometry with application to ILS glideslope', *IEEE Trans.*, 1976, **AP-24**, pp. 370–378
8 SENIOR, T.B.A.: 'The diffraction of a dipole field by a perfectly conducting half plane', *Q. J. Mech. & Appl. Math.*, 1953, **6**, p. 101
9 WOODS, B.D.: 'The diffraction of a dipole field by a half plane', *ibid.*, 1957, **10**, p. 90
10 BROMWICH, T.J.I.A.: *Proc. London Math. Soc.*, 1915, **14**, p. 450
11 BORN, M., and WOLF, E.: 'Principles of optics' (Pergamon Press, 1959), p. 108
12 KELLER, J.B.: 'Geometrical theory of diffraction', *J. Opt. Soc. Am.*, 1962, **52**, pp. 116–130
13 KELLER, J.B., LEWIS, R.M., and SECKLER, B.D.: 'Asymptotic solution of some diffraction problems', *Commun. Pure & Appl. Math.*, 1956, **9**, pp. 207–265
14 KOUYOUMJIAN, R.G., and PATHAK, P.H.: 'A uniform geometrical theory of diffraction for an edge in a perfectly conducting surface', *Proc. IEEE*, 1974, **62**, pp. 1448–1461
15 TIBERIO, R., and KOUYOUMJIAN: 'A uniform GTD analysis of diffraction by thick edges and strips illuminated at grazing incidence'. International Symposium on Antennas and Propagation Digest, University of Maryland, MD, USA, 1978
16 AHLUWALIA, LEWIS, R.M., and BOERSMA, J.: 'Uniform asymptotic theory of diffraction by a plane screen', *SIAM J. Appl. Math.*, 1968, **16**, pp. 783–807
17 LEE, S.W., and DESCHAMPS, G.A.: 'A uniform asymptotic theory of electromagnetic diffraction by a curved wedge', *IEEE Trans.*, 1976, **AP-24**, pp. 25–34
18 MITTRA, R., and RAHMAT-SAMII, Y.: 'A spectral domain analysis of high frequency diffraction problems' *in* USLENGHI, P.L.E. (Ed.): 'Electromagnetic scattering' (Academic Press Inc., 1978), pp. 121–183.
19 DESCHAMPS, G.A., BOERSMA, J., and LEE, S.W.: 'Three dimensional half plane diffraction: exact solution and testing of uniform theories', *IEEE Trans.*, 1984, **AP-32**, pp. 264–271
20 LUEBBERS, R., UNGVICHIAN, V., and MITCHELL, L.: 'GTD terrain reflection model applied to ILS glideslope', *IEEE Trans.*, 1982, **AES-8**, pp. 11–19
21 BREIEN, T.: 'Multipath analysis of ILS glidepath'. ELAB, N-7034, 1979
22 POULOSE, M.M., MAHAPATRA, P.R., and BALAKRISHNAN, N.: 'Accurate modelling of glideslopes for instrument landing system'. Proceedings of the International Conference on Radar, CICR-86, Nanjing, China, 4th–7th Nov. 1986, pp. 50–55
23 Manual on Testing of Radio Navigational Aids, ICAO, 11, Montreal, Canada.
24 LUEBBERS, R.J.: 'Finite conductivity uniform GTD versus knife edge diffraction in prediction of propagation path loss', *IEEE Trans.*, 1984, **AP-32**, pp. 70–76
25 POULOSE, M.M., MAHAPATRA, P.R., and BALAKRISHNAN, N.: 'Accurate prediction of terrain undulation and roughness effects in radiating systems'. Proceedings of the IEEE International Conference on Antennas and Propagation, Montreal, Canada, 29th Sept.–1st Oct. 1986